



## Photodegradation of flupentixol in aqueous solution under irradiation at 254 nm: Identification of the photoproducts generated

Aubert Maquille, Sybiline Salembier, Marie-France Hérent, Jean-Louis Habib Jiwan\*

Louvain Drug Research Institute, Université catholique de Louvain (UCL), 1200 Brussels, Belgium

### ARTICLE INFO

#### Article history:

Received 11 March 2010

Received in revised form 28 June 2010

Accepted 30 June 2010

Available online 8 July 2010

#### Keywords:

Flupentixol

Photolysis products

UHPLC

Mass spectrometry

MS<sup>n</sup>

### ABSTRACT

After irradiation at 254 nm of aqueous solutions of the antipsychotic drug flupentixol, the structures of the photodegradation products were determined by ultra high performance liquid-chromatography linked to mass spectrometry. Fragmentation patterns of the parent ions were established on a hybrid linear ion trap-orbitrap mass spectrometer allowing accurate mass measurements of both parent and daughter ions. This allowed to propose plausible structures for the main photolysis products of flupentixol. A total of nine photoproducts were detected after irradiation of the drug. The main photoproduct is generated following the addition of a hydroxyl group on the double bond adjacent to the thioxanthene ring. Secondary photoproducts were also observed.

© 2010 Elsevier B.V. All rights reserved.

### 1. Introduction

Many pharmaceuticals are sensitive to light, leading to a decrease in their purity and to the formation of photodegradation products. In addition, after the absorption of drugs, exposure to UV-A or UV-B irradiation in superficial areas in the body could lead to phototoxicity (caused by direct damage to the tissue induced by a photogenerated chemical agent) or photoallergic reaction (formation of an allergen such as a drug protein adduct) [1]. Stability tests on drugs, including light stress tests are required by the European Agency for the Evaluation of Medicinal Products [2] to assess the stability of the active substance.

Flupentixol is a thioxanthene drug, a class of typical antipsychotic used for the treatment of schizophrenic patients. Thioxanthene neuroleptics are photosensitive and are often responsible for photo-induced skin eruptions in patient treated with these drugs [3]. Detailed investigation on the identification of the photolysis products of this drug has not yet been carried on. The study of photodegradation products of such drugs may give insight onto the mechanisms leading to their formation.

Pharmaceuticals are released in the environment as a result from their use in human clinical practice and are commonly detected in the aquatic environment [4,5]. These compounds

exhibit biological activity which could affect aquatic biosystems and impact drinking water supplies. Photochemical reactions account for the degradation of pharmaceutical pollutants. Direct photolysis can also be used during drinking water treatment [6]. To some extent, photolysis at 254 nm can be extrapolated to environmental conditions [7,8], particularly concerning the structure of photoproducts. To this regard, the identification of the photolysis products of pharmaceuticals could improve the understanding of their environmental fate [9,10].

Hyphenated MS techniques have proven to be valuable tools for identifying drugs photolysis products [11,12]. The aim of this work is to identify degradation of flupentixol in aqueous solutions exposed to UV irradiation at 254 nm in order to define its photodegradation process. The UV spectrum of flupentixol in aqueous solution recorded in the wavelength region between 200 and 400 nm shows a maximum around 265 nm, which is close to the chosen irradiation wavelength. The main photolysis products were analyzed by LC-(MS)<sup>n</sup>. Quantification of the photoproducts was performed. Since standard compounds are not available this quantification is relative to the parent compound. This method of quantification is the recommended method by the European Agency for the Evaluation of Medicinal Products [13]. Structural characterizations of the main photolysis products were based on changes in molecular masses and spectral patterns of product ions. Accurate mass measurements and collision induced dissociation were carried on in a hybrid linear trap/orbitrap. Accurate mass measurement provides a higher grade of confidence for the assignment of the possible structure of the photodegradation products.

\* Corresponding author at: Université catholique de Louvain, Avenue E. Mounier, 72 bte 7230, B-1200 Brussels, Belgium. Tel.: +32 2 764 73 68; fax: +32 2 764 72 96.  
E-mail address: [j-l.habib@uclouvain.be](mailto:j-l.habib@uclouvain.be) (J.-L. Habib Jiwan).

## 2. Materials and methods

### 2.1. Materials

Cis-Z-flupentixol dihydrochloride (2-[4-[3-[2-(trifluoromethyl)thioxanthen-9-ylidene] propyl]piperazin-1-yl]ethanol) (>98% purity) was purchased from Sigma–Aldrich (St. Louis, MO, USA) and was stored in the dark. HPLC–MS grade methanol was supplied from Biosolve (Valkenswaard, Netherlands). Glacial formic acid was provided by Merck. Deionized water from a Millipore Milli-Q water purification system was used.

### 2.2. Samples

Three milliliters of flupentixol dihydrochloride  $0.5 \text{ mg ml}^{-1}$  solutions prepared with deionized water were put in quartz cells (1 cm path length) and irradiated in a Rayonet photochemical reactor equipped with four UV fluorescent lamps RPR 2537 Å. Air equilibrated solutions were exposed to UV irradiation for time intervals of 10, 15, 30, 45, 60, 90 and 180 min. Unirradiated control samples consisted in flupentixol solutions filled in quartz cells wrapped in aluminum foil and therefore, protected from light exposure. Experiments were performed at room temperature ( $293 \pm 4 \text{ K}$ ). All samples were protected from further light exposure after irradiation.

### 2.3. UHPLC–DAD–MS system

The LC MS/MS system consisted in a Thermo Accela pump, autosampler and photodiode array detector. Separation was performed on a Thermo Hypersil Gold C18 column,  $50 \text{ mm} \times 2.1 \text{ mm}$  packed with  $1.9 \mu\text{m}$  particle at a constant flow rate of  $500 \mu\text{l/min}$  using a binary solvent system: Solvent A, HPLC grade water with 0.1% formic acid and Solvent B, methanol. The initial HPLC gradient system was held at 15% B for 0.5 min then linearly increased to 90% B in 8 min, followed by a return to initial conditions for column re-equilibration. Analyses were performed in triplicate. The injection volume was  $5 \mu\text{l}$ . The absorbance was measured between 200 and 600 nm. The quantification wavelength was 265 nm. The MS system consisted of an LTQ–Orbitrap XL hybrid mass spectrometer (Thermo Fisher Scientific, Bremen, Germany) equipped with an electrospray ionization source. Mass spectrometry analyses were carried out in positive ion mode using full-scan MS with a mass range of 100–800  $m/z$ . The orbitrap operated at 30,000 resolution (full width at half height maximum, FWHM). All experimental data were acquired using external calibration prior to data acquisition. Data acquisition and processing was carried out with Xcalibur 2.0.7 software (Thermo). The mass parameters were as follows: capillary temperature:  $250^\circ\text{C}$ ; sheath and auxiliary gas flow 40 and 20 arbitrary units, respectively; source voltage: 5 kV; capillary voltage: 8 V; tube lens voltage: 40 V. Collision induced dissociation experiments were carried out at 40% normalized collision energy.

### 2.4. Validation studies

Quantification of all peaks was based on UV detection. The percentage of flupentixol remaining after UV exposure was calculated from the ratio of the areas under the curve of the drug peak between irradiated and control samples [14].

The photolysis products were quantified as a percentage of the initial drug concentration. As no standards were available for these products, and according to the guidelines [15], they were quantified as flupentixol, assuming they have similar response factors as the parent drug. Flupentixol solutions in concentrations ranging from 2 to  $200 \mu\text{M}$  were injected in order to establish the calibration curve (six calibration points). The calibration curve was constructed by

plotting the peak areas (measured in nominal units) against the corresponding flupentixol concentration. The obtained relationship was the following:  $y = 8167x - 7$ ,  $r^2 = 0.998$ . Standard deviation of the slope was 16 whilst standard deviation of the intercept was 1581. The limits of detection (LOD) and quantification (LOQ), considered, respectively, as 3 and 10 times the signal-to-noise ratio [14], were evaluated by injecting progressive dilutions of flupentixol into the LC system. LOQ was  $2 \mu\text{M}$ .

Repeatability and reproducibility were evaluated by analyzing the same standard solution three times on the same day and preparing and analyzing standard solutions at similar concentration on three different days. The observed RSD for intraday variation was about 1.5%. The inter-day RSD was about 2%.

## 3. Results and discussion

### 3.1. Photodegradation of flupentixol

Fig. 1 represents the remaining flupentixol concentration as a function of the irradiation time. The logarithmic plot of the flupentixol as a function of time up to 60 min of irradiation inserted in Fig. 1 shows that the photolysis degradation of flupentixol at 254 nm follows first-order kinetics up to that time of irradiation. Regression analysis gave a high correlation coefficient, demonstrating the validity of the first-order kinetic. Under these conditions, a rate constant,  $k$ , of  $0.0096 \text{ min}^{-1}$  and a half-time,  $T_{1/2}$ , of 72.2 min are obtained. Fast degradation of flupentixol occurs following irradiation. Only 55% of the initial drug concentration remains after a 60 min irradiation. However, for longest irradiation times, the remaining concentration is higher than expected (e.g. about 40% of the drug is still present after a 180 min irradiation) which may be due to a quenching of the photolysis products.

### 3.2. Photodegradation products

An overlay of the UV chromatograms of photo-irradiated flupentixol is shown in Fig. 2. The quantification results for the main photolysis products expressed as percentages of the initial drug concentration are reported in Table 1. The degradation peaks were numbered by increasing retention times.

Peak 4 was already present in control unirradiated samples and did not increase significantly following UV irradiation. A total of 10 degradation peaks are detected after irradiation of flupentixol.

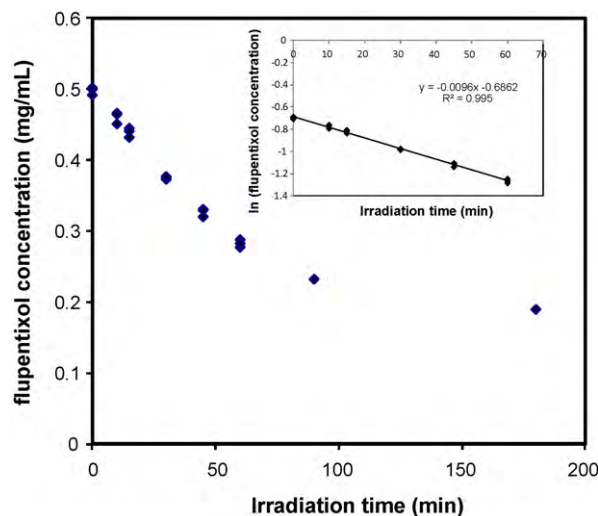


Fig. 1. Evolution of the concentration of flupentixol as a function of irradiation time. Insert: first-order kinetic plot for the photo-induced degradation of flupentixol up to 60 min.

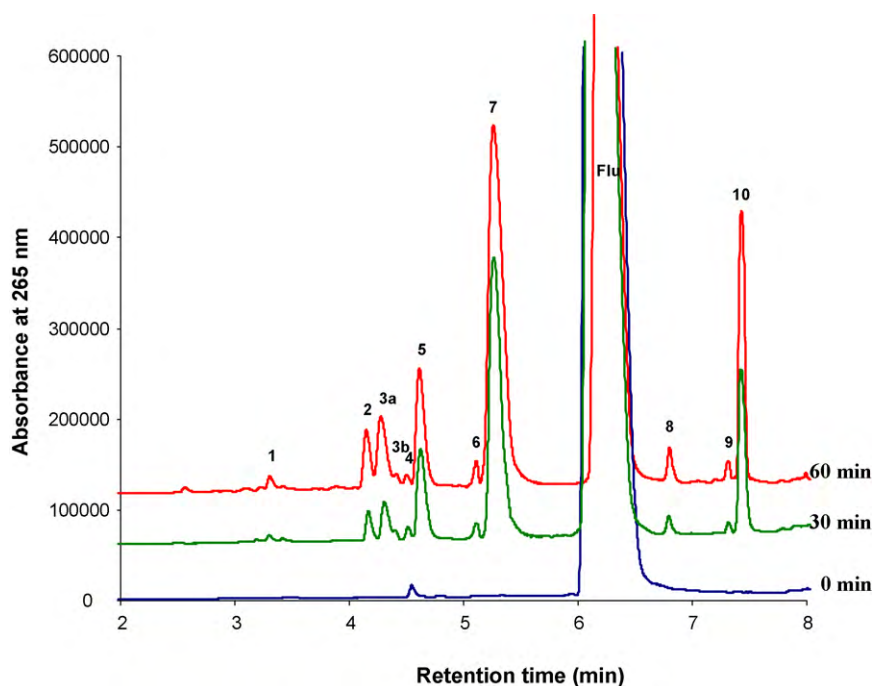


Fig. 2. Overlay of UHPLC-UV chromatograms of flupentixol solutions  $0.5 \text{ mg ml}^{-1}$  obtained at increasing irradiation times.

The most intense degradation peak (7) accounts for about 18% of the initial parent drug concentration after 60 min irradiation. The concentration of all photolysis products increased up to 90 min irradiation although at 60 min, a decrease is observed for peak 7 which is the major degradation peak. This decrease may be attributed to the photolysis of this compound, leading to secondary photolysis products.

### 3.3. Characterization of photolysis products

Identification of photolysis products was performed by liquid-chromatography coupled to a linear ion trap–orbitrap mass spectrometer that allows collision induced dissociation (CID) and accurate mass determination on both product ions and precursors. This enables to determine the empirical formula for the unknown photolysis products. The relative mass errors were below 2 ppm which guarantees the correct assignment in all the cases. Using an electrospray ionization source and detection in the positive mode, pseudo-molecular ions  $[M+H]^+$  have been obtained for each compound. Collision induced dissociation was performed on each photolysis product in order to confirm the proposed structure. A comparison of the fragmentation pattern of the photoproducts with that of flupentixol allowed to assign the location of the modifica-

tion. Mass accuracy measurements allowed the assignment of the molecular formula of product ions.

Fig. 3 shows the collision induced dissociation mass spectrum of flupentixol together with its major fragments. CID of flupentixol yields to three fragments ions at mass-to-charge ratios ( $m/z$ ) of 390 (resulting from the loss of  $C_2H_5O$  from the lateral chain), 307 originating from the loss of the hydroxyethylpiperazine ring and 362 (corresponding to the breakage of the piperazine ring). A  $m/z$  265 ion ( $C_{14}H_8F_3S$ ) corresponds to the loss of the whole lateral chain. Consecutive losses of hydrofluoric acid are observed and lead to  $m/z$  415, 395 and 375 daughter ions. A  $m/z$  169 fragment that corresponds to the whole lateral chain is also present. All the proposed structures of the fragment ions were consistent with the results from the accurate mass measurement.

The exact masses of flupentixol and its photolysis products as well as the corresponding formula are listed in Table 2. The main CID fragments for photolysis products and their daughter ions are reported in Table 3. The structures of the photolysis products are shown in Fig. 4.

Three isobaric compounds with  $m/z$  451 are detected at 4.4, 4.5 and 6.8 min (products 3b, 4 and 8). These compounds correspond to the addition of an oxygen atom on the parent drug. Slight differences are observed in their MS–MS fragmentation patterns. The

Table 1

Quantification of the degradation peaks generated following UV irradiation of flupentixol  $0.5 \text{ mg ml}^{-1}$  solution at different times.

Peak	Products	R.T. (min)	Mean percentages of impurity peaks relative to the initial drug concentration						
			0 min	10 min	15 min	30 min	45 min	60 min	90 min
1	(1)	3.35	<LOD	<LOQ	0.29	0.37	0.52	0.65	1.55
2	(2)	4.15	<LOD	0.70	0.81	1.54	2.26	2.80	4.04
3	(3a) (3b)	4.35	<LOD	0.34	0.79	1.69	2.37	3.15	6.96
4	(4)	4.49	0.77	0.67	0.64	0.67	0.66	0.74	0.75
5	(5)	4.61	<LOD	1.77	2.57	2.94	3.58	4.54	7.78
6	(6)	5.12	<LOD	0.56	0.75	1.03	1.24	1.39	1.50
7	(7)	5.27	<LOD	7.76	10.22	14.34	16.29	18.32	14.72
8	(8)	6.82	<LOD	0.35	0.48	0.75	1.04	1.42	2.46
9	(9)	6.26	<LOD	<LOQ	0.31	0.36	0.42	0.64	0.95
10	(10)	7.43	<LOD	1.64	2.43	3.62	4.90	6.98	13.38

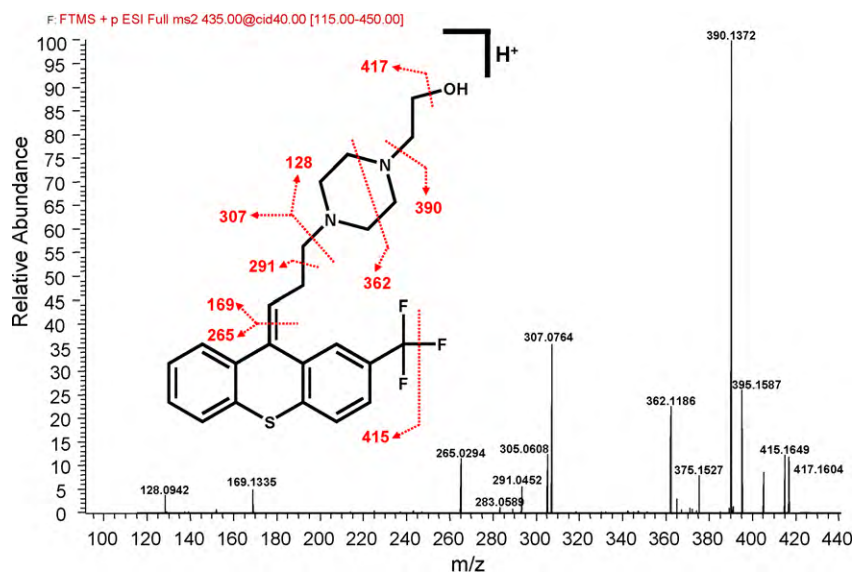


Fig. 3. MS–MS spectra and structure of flupentixol and its fragment ions.

first product (3b) shows fragments such as 169 and 143 that correspond to an intact lateral chain. In addition it exhibits a  $m/z$  281 fragment that corresponds to the ring containing an oxygen. Therefore, this product might be formed following oxidation of the sulfur into a S-oxide such as it is the case for many sulfide containing drugs such as diltiazem [16].

The fragmentation of the two other products does not indicate the presence of an oxygen on the ring. The presence of a  $m/z$  293

ion amongst the daughter ion of product (4) shows that the oxygen is located on the first part of the lateral chain. Product (4) does not increase following irradiation so that it could not be considered as a photoproduct. For product (8), the  $m/z$  421 fragment results from the loss of a  $\text{CH}_2\text{O}$  moiety, which differs from the fragmentation pattern of flupentixol. The  $m/z$  307 fragment shows that the modification is located on the piperazine part. This product might result from the cleavage of the piperazine ring according to a mech-

Table 2

List of experimentally measured accurate mass of flupentixol and its photodegradation products with the predicted mass-to-charge values for the proposed chemical formula and the relative mass error.

Product no.	Chemical formula	Experimental mass	Theoretical mass	Mass error (ppm)
1	$\text{C}_{21}\text{H}_{24}\text{O}_2\text{N}_2\text{F}_3\text{S}$	425.15005	425.15051	−1.08
2	$\text{C}_{23}\text{H}_{29}\text{O}_4\text{N}_2\text{S}$	429.18378	429.18425	−1.11
3a	$\text{C}_{21}\text{H}_{26}\text{O}_2\text{N}_2\text{F}_3\text{S}$	427.16569	427.16616	−1.1
3b	$\text{C}_{23}\text{H}_{26}\text{O}_2\text{N}_2\text{F}_3\text{S}$	451.16577	451.16616	−0.86
4	$\text{C}_{23}\text{H}_{26}\text{O}_2\text{N}_2\text{F}_3\text{S}$	451.16578	451.16616	−0.84
5	$\text{C}_{23}\text{H}_{28}\text{O}_3\text{N}_2\text{F}_3\text{S}$	469.17602	469.17672	−1.5
6	$\text{C}_{21}\text{H}_{24}\text{ON}_2\text{F}_3\text{S}$	409.15512	409.1556	−1.16
7	$\text{C}_{23}\text{H}_{28}\text{O}_2\text{N}_2\text{F}_3\text{S}$	453.18101	453.18181	−1.77
8	$\text{C}_{23}\text{H}_{26}\text{O}_2\text{N}_2\text{F}_3\text{S}$	451.16552	451.16616	−1.42
9	$\text{C}_{16}\text{H}_{10}\text{OF}_3\text{S}$	307.03962	307.0399	−0.9
10	$\text{C}_{14}\text{H}_8\text{OF}_3\text{S}$	281.02411	281.02425	−0.49
Flupentixol	$\text{C}_{23}\text{H}_{26}\text{ON}_2\text{F}_3\text{S}$	435.17044	435.17125	−1.85

Table 3

List of MS–MS fragments and daughter ion fragments for the main photoproducts of flupentixol.

Product no.	Experimental mass	Theoretical mass	Mass error (ppm)	Fragmentation
1	425.15005	425.15051	−1.08	409.1556 364.0982 338.0820 281.0245
2	429.18378	429.18425	−1.11	MS3 of 409 411.1734 299.0736 143.1176
3a	427.16569	427.16616	−1.1	409.1555 391.1449
3b	451.16577	451.16616	−0.86	MS3 of 409 391.1449 348.1028 322.0871 307.0760 265.0293
4	451.16578	451.16616	−0.84	433.1555 321.0562 281.0244 169.1335 143.1178
5	469.17602	469.17672	−1.5	433.1555 406.1321 293.0244 265.0294 143.1177
6	409.15512	409.1556	−1.16	451.1659 433.1556 339.0661 157.1334
7	453.18101	453.18181	−1.77	MS3 of 339 321.0556 297.0193 281.0242
8	451.16552	451.16616	−1.42	391.1449 348.1028 322.0871 307.0762 265.0293
9	307.03962	307.0399	−0.9	435.1711 323.0712 295.0393 281.0243 265.0294
10	281.02411	281.02425	−0.49	433.1555 421.1555 364.09774 307.0763 265.0294
				287.0337 279.0450 265.0293 238.0446
				261.0179 233.0230 212.0288 184.0339

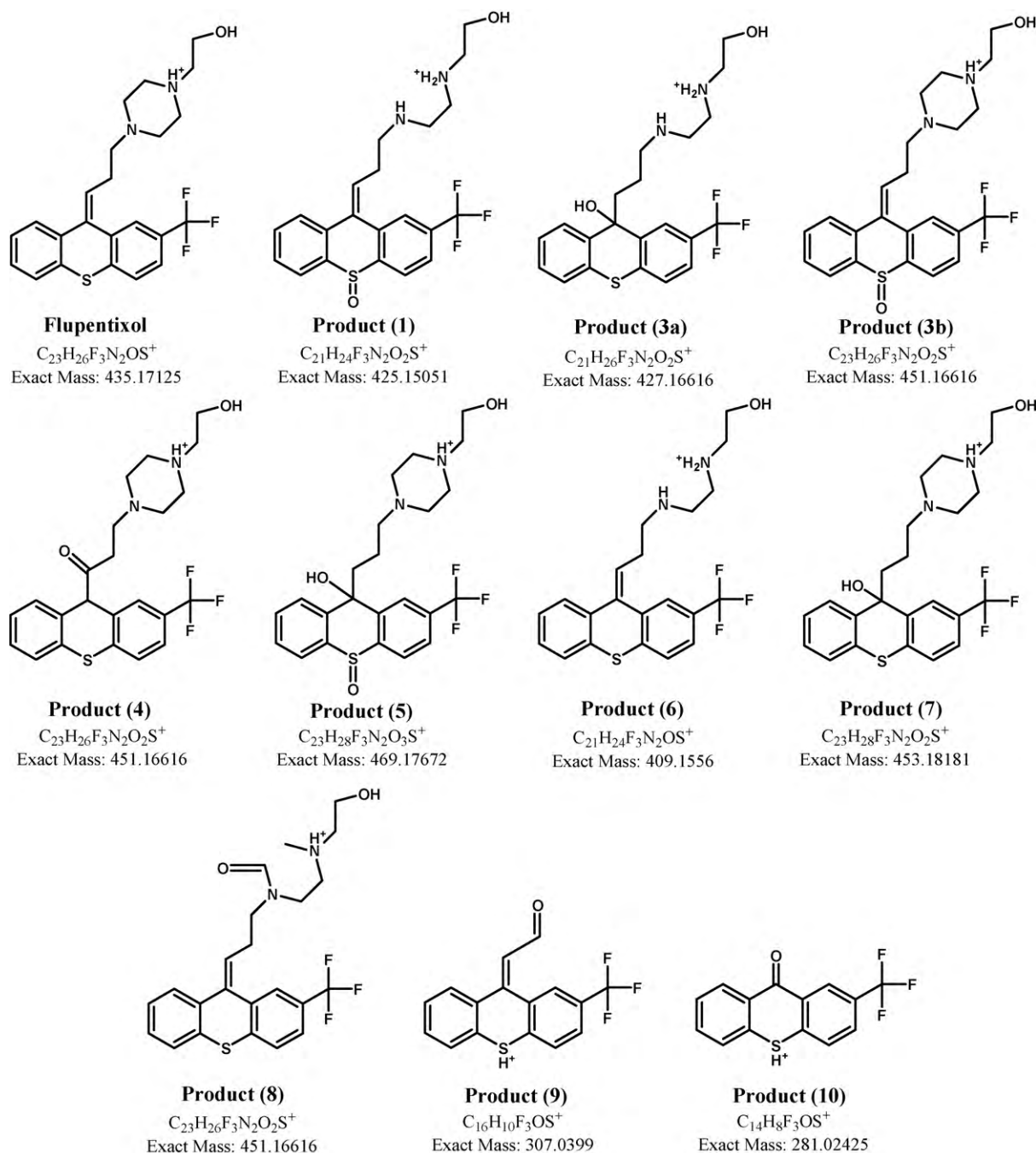


Fig. 4. Structures of flupentixol and its main photolysis products (protonated).

anism proposed by Mella et al. [18]. The  $m/z$  364 ion corresponds to  $C_{19}H_{17}F_3NOS$ .

Product (10) with  $m/z$  281 corresponds to the formula  $C_{14}H_8F_3S$ . Its main fragments fragment with  $m/z$  261 results from the loss of hydrofluoric acid whereas  $m/z$  212 originates from the loss of the  $CF_3$  group. The  $m/z$  233 fragment is due to the losses of both HF and CO which may indicate the presence of a ketone within this molecule. This product would result from oxidation of flupentixol into a thioxanthone ring.

Product (9), with  $m/z$  307 corresponds to the formula  $C_{16}H_{10}OF_3S$ . CID this product leads to the losses of HF ( $m/z$  287),  $CF_3$  ( $m/z$  238) and CO ( $m/z$  279). The presence of the  $m/z$  265 ion indicates that the thioxanthene ring is intact. Therefore, the modification is located on the lateral chain which is consistent with the proposed structure.

The formula  $C_{21}H_{24}ON_2F_3S$  was assigned to product (6), which differs from the parent compound by the loss of acetylene. The 265  $m/z$  fragment indicates that the thioxanthene ring was not modified. Comparison of the MS–MS spectra of this photoproduct with that of flupentixol determined that the modification was located on the piperazine ring as the presence of  $m/z$  307 amongst the fragments indicated that the first part of the lateral chain is intact. In addition, the loss of 61.0523 mass units to yield  $m/z$  348 product ion corresponds to the loss of 2-aminomethanol from the lateral chain. Therefore, the modification corresponds to N-dealkylation of the ring following UV irradiation. The breakage of the piperazine ring has also been reported for other drugs such as ciprofloxacin [17,18].

Fragmentation of product 3a ( $m/z$  427) gives a  $m/z$  409 fragment. Fragments originating from MS<sup>3</sup> fragmentation of this daughter

ion are identical to those obtained after CID of product (6). Therefore, these two products only differ by the addition of a hydroxyl together with the reduction of a double bond. This product might be a secondary photoproduct originating from the photolysis of product (7) since a significant increase of its corresponding peak is observed at long irradiation times.

The  $m/z$  453 product originates from the addition of a hydroxyl on the molecule and from the reduction of a double bond. CID of this product leads to losses of water ( $m/z$  435), the  $m/z$  323 fragment correspond to the breakage between the carbon and the piperazine ring, indicated no changes on this part of the lateral chain. The  $m/z$  281 product, with a formula of  $C_{14}H_8OF_3S$ , indicates the presence of an oxygen on the thioxanthene ring although the fragment  $m/z$  265 results from the loss of that oxygen together with the whole lateral chain. Therefore, this product could correspond to the addition of a hydroxyl radical on the double bond from the lateral chain. Due to its higher electrophilicity, the addition is favored on the ternary carbon from the thioxanthene ring to give product (7).

Product (5) corresponds to the addition of two oxygen atoms on the parent drug together with the reduction of a double bond. Fragmentation of this product into a  $m/z$  339 ion indicates that the piperazineethanol part was not modified. The  $m/z$  297 fragment corresponds to the loss of  $C_9H_{20}N_2O$ , which is the whole lateral chain. Therefore, the modification has occurred on the ring and may correspond to addition of a hydroxyl on the double bond adjacent to the ring together with oxidation of the sulfur into a S-oxide.

The exact structure of product (2) could not be determined. It contains no fluoride and its fragmentation pattern indicates that the lateral chain is the same as the parent drug. The position of the three oxygen atoms on the ring could not be determined by mass spectrometry.

The fragmentation of product (1) with a  $m/z$  of 425 fragments results in the formation of daughter ions with  $m/z$  of 409 (loss of water), 364 ( $C_{19}H_{17}F_3NOS$ ), 338 and 281. This later fragment indicates the presence of an oxygen on the ring. The fragmentation pattern is concordant with the breakage of the piperazine ring together with oxidation of the sulfur from the thioxanthene ring.

### 3.4. Photolysis mechanisms

The main photodegradation mechanism of flupentixol appears to be due to the addition of a hydroxyl group on the double bond adjacent to the ring to give product (7). The decrease in the concentration of this product after long irradiation times indicates that it also undergo photolysis into secondary photoproducts such as products (3a) and (5) whose corresponding peaks appears to increase.

In the proposed structures of the photolysis products, no breakdown of the thioxanthene ring is observed which suggest that the photolytic process do not lead to complete photomineralization of the drug. The attack of oxygen on the sulfur is commonly observed following UV irradiation although in the case of flupentixol it accounts only for a small portion of the drug degradation, contrary to other sulfur containing cycles such as diltiazem for which the S-oxide was the major degradation product [16].

The breakage of the piperazine ring following UV irradiation has already been described for ciprofloxacin by Mella et al. [18]. This reaction necessitates hydrogen abstraction from the ring followed by the attack of water on the radical and hydrogen transfer to give an aldehyde that may correspond to product (8). According to this mechanism, further photolysis of product (8) leads to product (6), which is a secondary photoproduct.

The phototoxicity and the photoallergic reaction of the drug could be explained by the formation of photolysis products such as products (9) or product (10) with aldehyde and ketones that could readily react with proteins following degradation of the drug in the superficial layer of the body.

## 4. Conclusions

Flupentixol is rapidly degraded upon UV irradiation of solutions up to ca. 60%. At that point, the concentration of the photoproducts in the solution is certainly sufficiently high to compete with flupentixol for light absorption and photoreaction. The major photodegradation pathway occurs through hydroxyl addition on the double bond. For the majority of the photoproducts, the thioxanthene ring remains intact although oxidation into thioxanthone was observed for three minor products.

## Acknowledgments

The authors would like to thank the Belgian National Fund for Scientific Research (FNRS) (FRFC 2.4555.08), the Special Fund for Research (FSR) and the faculty of medicine of UCL for their financial support for the acquisition of the LTQ-Orbitrap.

## References

- [1] G. Cosa, Photodegradation and photosensitization in pharmaceutical products: assessing drug phototoxicity, *Pure Appl. Chem.* 76 (2004) 263–275.
- [2] European Agency for the Evaluation of Medicinal Products (EMA), Photostability testing of new active substances and medicinal products, ICH Topic Q1B, step 5 (CPMP/ICH/279/95), EMA, London, 1995.
- [3] B. Eberlein-König, A. Bindl, B. Przybilla, Phototoxic properties of neuroleptic drugs, *Dermatology* 194 (1997) 131–135.
- [4] M. Petrović, M.D. Hernando, M.S. Díaz-Cruz, D. Barceló, Liquid chromatography–tandem mass spectrometry for the analysis of pharmaceutical residues in environmental samples: a review, *J. Chromatogr. A* 1067 (2005) 1–14.
- [5] O.A. Jones, N. Voulvoulis, J.N. Lester, Human pharmaceuticals in the aquatic environment a review, *Environ. Technol.* 22 (2001) 1383–1394.
- [6] O. González, C. Sans, S. Espulgas, S. Malato, Application of solar advanced oxidation processes to the degradation of the antibiotic sulfamethoxazole, *Photochem. Photobiol. Sci.* 8 (2009) 1032–1039.
- [7] A.L. Boreen, W.A. Arnold, K. McNeill, Photochemical fate of sulfa drugs in the aquatic environment: sulfa drugs containing five-membered heterocyclic groups, *Environ. Sci. Technol.* 38 (2004) 3933–3940.
- [8] D. Błędzka, D. Grygliński, J.S. Miller, Photodegradation of butylparaben in aqueous solutions by 254 nm irradiation, *J. Photochem. Photobiol. A: Chem.* 203 (2009) 131–136.
- [9] A. Píram, A. Salvador, C. Verne, B. Herbreteau, R. Faure, Photolysis of beta-blockers in environmental waters, *Chemosphere* 73 (2008) 1265–1271.
- [10] B.L. Edlund, W.A. Arnold, K. McNeill, Aquatic photochemistry of nitrofurantoin antibiotics, *Environ. Sci. Technol.* 40 (2006) 5422–5427.
- [11] C. Sirtori, A. Zapata, S. Malato, W. Gernjak, A.R. Fernández-Alba, A. Agüera, Solar photocatalytic treatment of quinolones: intermediates and toxicity evaluation, *Photochem. Photobiol. Sci.* 8 (2009) 644–651.
- [12] A. Maquille, J.-L. Habib-Jiwan, LC–MS characterization of photolysis products from UV irradiated metoclopramide solutions, *J. Photochem. A: Chem.* 205 (2009) 197–202.
- [13] European Agency for the Evaluation of Medicinal Products (EMA), Note for guidance on impurities in new medicinal products, Topic Q3B, step 4 (CPMP/ICH/2738/99), London, 2006.
- [14] European Pharmacopoeia, 5th edition, Council of Europe, Strasbourg, 2005.
- [15] European Agency for the Evaluation of Medicinal Products (EMA), Note for guidance on impurities in new medicinal products, Topic Q3B, step 4 (CPMP/ICH/282/95), London, 1996.
- [16] V. Andrisano, P. Hrelia, R. Gotti, A. Leoni, V. Cavrini, Photostability and phototoxicity studies on diltiazem, *J. Pharm. Biomed. Anal.* 25 (2001) 589–597.
- [17] T.G. Vasconcelos, D.M. Henriques, A. König, F.A. Martins, K. Kümmerer, Photodegradation of the antimicrobial ciprofloxacin at high pH: identification and biodegradability assessment of the primary by-products, *Chemosphere* 76 (2009) 487–493.
- [18] M. Mella, E. Fasani, A. Albini, Photochemistry of 1-cyclopropyl-6-fluoro-1,4-dihydro-4-oxo-7-(piperazin-1-yl)quinoline-3-carboxylic acid (=ciprofloxacin) in aqueous solution, *Helv. Chim. Acta* 84 (2001) 2508–2519.